ELSEVIER

Inorganica Chimica Acta 226 (1994) 275–283

Inorganica Chimica Acta

# Oxidative quenching of luminescence from copper metallothionein

Anna Rae Green, Martin J. Stillman *

*Department of Chemistry, University of Western Ontario, London, Ont., N6A 5B7, Canada*

Received 1 July 1994

**Abstract**

Mammalian metallothioneins readily bind up to 20 Cu(I); with a two domain structure involving $Cu_6(S_{cys})_{11}$ ($\alpha$) and $Cu_6(S_{cys})_9$ ($\beta$) copper–thiolate clusters proposed for the $Cu_{12}$-MT species. Copper metallothioneins luminesce in the 600 nm region when excited by 300 nm light. The 300 nm Stokes' shift and the dependence of the 600 nm emission band entirely on the presence of Cu(I) provides a sensitive probe of the copper–thiolate cluster structures that form the Cu(I) binding site in $Cu_n$-MT, where $n = 1$–12. Luminescence quenching data for the emissive Cu(I) state were used to monitor electron transfer in copper metallothionein. CD spectral data measured together with the emission spectrum show that the three-dimensional structure of the protein is maintained even when the excited state is completely quenched by molecular oxygen. Different acrylamide quenching rates for $(Zn_4)_\alpha(Cu_6)_\beta$-MT and $(Cu_6)_\alpha(Cu_6)_\beta$-MT suggest that structural differences dependent on the Cu(I) loading, especially the occupation of one or both domains by Cu(I), may influence the excited state properties of copper-containing mammalian metallothioneins. Finally, Fe(III) is efficiently reduced to Fe(II) following oxidative quenching of the luminescence of the $Cu_{12}$-MT; CD spectroscopy shows that the three-dimensional structure of $Cu_{12}$-MT is destroyed.

*Keywords:* Copper metallothionein; Oxidative quenching; CD spectroscopy; Luminescence quenching

## 1. Introduction

Metallothionein is a ubiquitous protein with a wide range of proposed physiological roles, including the transport, storage and detoxification of essential and non-essential trace metals [1–3]. Fig. 1 shows the amino acid sequence of the isoform of rabbit metallothionein used in the following study. With 20 cysteinyl groups out of 60–62 amino acids in the peptide chain, mammalian metallothionein represents an impressive chelating agent for a wide range of metals. Structural studies have been carried out using $^1H$ and $^{113}Cd$ NMR, X-ray crystallography, optical spectroscopy and more recently EXAFS [4–9]. Three structural motifs have been identified for metal binding to mammalian metallothioneins. These three structures are defined by specific metal to protein stoichiometric ratios and depend on the coordination geometry adopted by the metal in the metal binding site. The $M_7$-MT (M = Zn(II), Cd(II), Hg(II)) [4–8,10], $M_{11\text{-}12}$-MT (M = Ag(I), Cu(I), Hg(II)) [4,10–14], and $M_{17\text{-}18}$-MT (M = Hg(II), Ag(I)) [4,14–16] clustered structures that form in the metal binding site(s) in mammalian metallothioneins have been associated, respectively, with tetrahedral, trigonal and digonal coordination geometries around the metal. The $M_7$-MT species has been completely characterized for M = Cd(II) and Zn(II). $^{113}Cd$ NMR and X-ray crystallography data show that $Cd_7$-MT and $Zn_7$-MT have a two domain structure, with metal–thiolate clusters of the form $M_4(S_{cys})_{11}$ (the $\alpha$ domain) and $M_3(S_{cys})_9$ (the $\beta$ domain) (see Fig. 2) [5–8]. A similar two domain structure involving $Cu_6(S_{cys})_{11}$ ($\alpha$) and $Cu_6(S_{cys})_9$ ($\beta$) copper–thiolate clusters has been proposed for the $Cu_{12}$-MT species [11–13]. Analysis of EXAFS data has suggested that these copper(I)–thiolate clusters are formed with trigonal $CuS_3$ units [17,18].

The luminescence spectrum of copper metallothioneins in the 600 nm region is well known [19–27] and has been attributed to a transition from excited triplet, metal-based states that are populated by absorption into the 260–300 nm region of the metal–thiolate charge transfer states [27]. The 300 nm Stokes' shift and the dependence of the 600 nm emission band entirely on

* Corresponding author. Tel: (519) 661-3821; Fax: (519) 661-3022; Internet: stillman@uwo.ca.


*SSDI* 0020-1693(94)04096-E

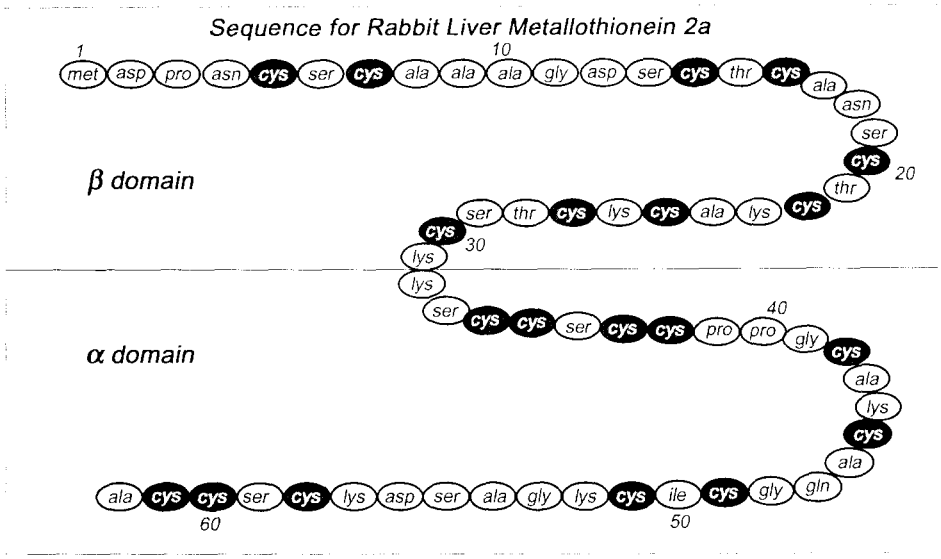


Fig. 1. Amino acid sequence of isoform 2a of metallothionein isolated from rabbit liver as cited in Ref. [46]. The twenty cysteine residues (Cys) are shaded in black. The $\beta$ domain is located at the –N terminal of the protein and consists of residues 1–31 while the $\alpha$ domain is located at the –C terminal and consists of residues 32–62.

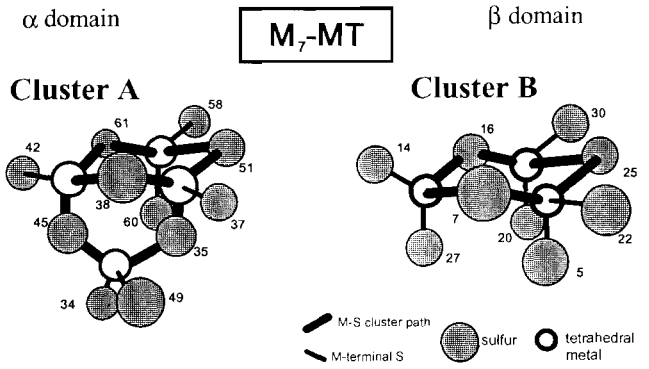


Fig. 2. Three-dimensional structure of the metal–thiolate clusters in $M_7$-MT (M = Zn, Cd) based on the data of Refs. [5–8]. The shaded atoms represent the sulfur atoms of the cysteine residues in the protein backbone as shown in Fig. 1. The white atoms represent a tetrahedrally bound Zn(II) or Cd(II) metal. Cluster A ($M_4(S_{cys})_{11}$) is found in the $\alpha$ domain and cluster B ($M_3(S_{cys})_9$) is found in the $\beta$ domain.

the presence of Cu(I) provides a sensitive probe of the copper–thiolate cluster structures that form the Cu(I) binding site in $Cu_n$-MT, when $n = 1$–12.

In this paper we use the quenching of the emissive Cu(I) state to monitor electron transfer in copper metallothionein. In previous studies [11] we have demonstrated how the $Cu_6S_{9/11}$ clusters are insulated from the solvent by the surrounding peptide chain. This structural feature offers several possibilities for electron transfer under controlled conditions.

For example for cluster B: oxidation $[Cu(I)_6S_9]^{3-} \Longleftrightarrow [Cu(I)_5Cu(II)S_9]^{2-} + e^-$ or reduction $e^- + [Cu(I)_6S_9]^{3-} \Longleftrightarrow [Cu(I)_5Cu(0)S_9]^{4-}$.

## 2. Experimental

$Zn_7$-MT was isolated from rabbit livers following in vivo induction procedures using aqueous zinc salts. The protein was purified using gel filtration and electrophoresis as previously described [28,29]. Although both isoforms (MT 1 and MT 2) were isolated, only isoform 2 was used in the experiments described here.

Aqueous protein solutions were prepared by dissolving the protein in argon-saturated distilled water. Protein concentrations were estimated from measurements of the –SH group and zinc concentrations as described previously. These estimations were based on the assumption that there are 20 –SH groups and 7 Zn atoms in each protein molecule. The concentration of –SH groups was determined by the spectrophotometric measurement of the colored thionitrobenzoate anion ($\epsilon_{420} = 13\,600\ M^{-1}\ cm^{-1}$) produced by reaction with DTNB (5,5′-dithiobis(-2-nitrobenzoic acid)) in the presence of 6 M guanidine hydrochloride [30]. Zinc concentrations were determined by flame atomic absorption spectroscopy (AAS) using a Varian model 875 atomic absorption spectrophotometer with a Varian model 55 programmable sample changer.

Samples of 2 or 3 ml of 10 $\mu$M aqueous $Zn_7$-MT 2 were titrated with $\mu$l aliquots of Cu(I) in the form of $[Cu(CH_3CN)_4]ClO_4$. This salt was prepared by the method of Hemmerich and Sigwart [31] and was dissolved in a 30% (vol./vol.) acetonitrile/water solution. Unless stated otherwise, protein solutions were bubbled with Ar for 5 min after each addition of Cu(I) before the spectral data were measured. The preparation of all samples using argon-saturated solutions produces samples with the same luminescent intensities and

lifetimes as those samples subjected to freeze–thaw cycles.

Emission spectra and decay data were measured on a Photon Technology Inc. LS-100 spectrometer. Circular dichroism spectra were recorded on a Jasco J-500C spectropolarimeter controlled by an IBM S9001 computer using the program CDSCAN [32]. The temperature of the emission and CD experiments was controlled using Endocal circulating baths to pump a 50% ethylene glycol/water mixture around the cell compartments. UV–Vis absorption spectra were recorded on an AVIV mode 17DS UV–Vis–IR spectrophotometer. For observation of emission in the 500–700 nm region with excitation at 300 nm, optical glass filters were placed over the excitation (Corning 7-54 or Schott BG-24) and emission slits (Corning CS 3-74 or Schott GG-420). All spectral data were organized and plotted using the program Spectra Manager [33]).

## 3. Results and discussion

### 3.1. Emissive properties of copper-substituted metallothionein

Many metals will bind to apo-MT (metal-free metallothionein) or will displace Zn(II) bound to Zn-MT in vitro [1,2]. When Cu(I) is added to solutions of apo-MT or $Zn_7$-MT, an emission band appears near 600 nm when the solution is excited at 300 nm at both room temperatures (0–50 °C) and cryogenic temperatures (77 K) [11,27]. This emission is long lived ($\tau$ in the $\mu$s range) and is entirely dependent on the presence of the bound Cu(I). Fig. 3 shows the dependence of the $\lambda_{max}$ and intensity of this emission band on the degree of Cu(I) loading at 40 °C. A single sample of aqueous rabbit liver $Zn_7$-MT was titrated with mol equiv. (1 mole Cu(I) per mole protein) aliquots of Cu(I) at pH 6.6. As seen in Fig. 3(A), the emission intensity increases as 0–12 Cu(I) are added, with the most dramatic increases occurring for the 8th through 12th additions of Cu(I). Fig. 3(B) shows that in aqueous solutions the emission intensity decreases towards zero when 13–20 Cu(I) are added. In previous studies [11], we have associated the trend observed for between 1 and 12 Cu(I) with the formation of a $Cu_{12}$-MT species $(Cu_6)_\alpha(Cu_6)_\beta$-MT in which the two Cu(I)–thiolate clusters are efficiently shielded from the solvent by the peptide backbone. We have proposed [11] that the addition of more Cu(I) (from 13 to 20 Cu(I)) causes the peptide backbone to unwind to accommodate the additional Cu(I) until 1 Cu(I) is ligated by a single cysteinyl thiolate in $Cu_{20}$-MT. The reaction between rabbit liver metallothionein and Cu(I) when Cu(I) > 12 is completely reversible. If stoichiometric amounts of $Zn_7$-MT are subsequently added to a solution nominally

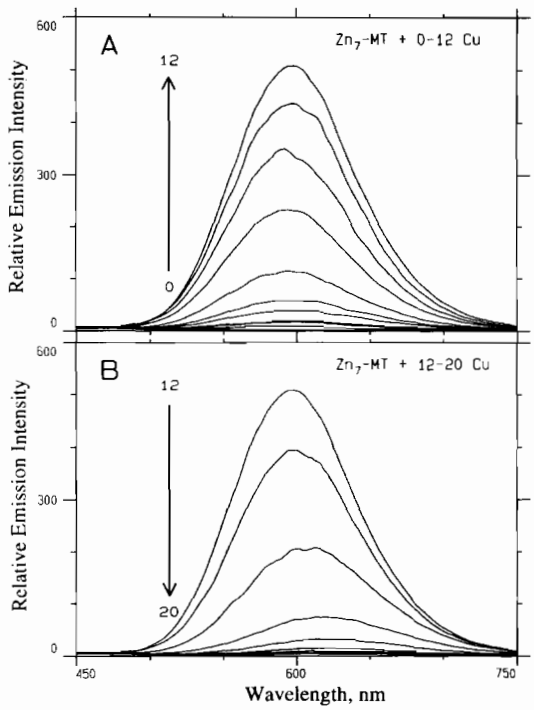


Fig. 3. Emission spectra recorded (following excitation at 300 nm) as Cu(I) is added to a 10 $\mu$M aqueous solution of $Zn_7$-MT at 40 °C. Each line represents the spectrum recorded following sequential additions of a single mol equiv. of Cu(I). The emission intensity increases as 0–12 mol equiv. of Cu(I) is added to the protein solution (A), and then decreases with further additions of Cu(I) (B).

written as $Cu_{15}$-MT, a greater concentration of $Cu_{12}$-MT can be formed and the emission intensity is restored to the values expected for $Cu_{12}$-MT. Clearly, the Cu(I) redistributes between all available protein. This result also demonstrates that under our conditions Cu(I) in excess of 12 Cu(I):MT binds to the protein and is not involved in disproportionation reactions that would form Cu(II) and Cu(0). We find no evidence for oxidation of the cysteinyl thiolates to form disulfide bonds ($2RS^- \Rightarrow RS\text{–}SR$) or oxidation of the Cu(I) bound to the protein. If the $Cu_{12}$-MT species is formed in a 50% (vol./vol.) acetonitrile/water solvent mixture, the acetonitrile will compete for the Cu(I) past the 12 Cu(I) point and the $Cu_{20}$-MT species does not form [34].

As seen in Fig. 3(A), the addition of only 6 Cu(I) to $Zn_7$-MT results in an emission spectrum which is much less intense than that of $Cu_{12}$-MT. At the high temperature (40 °C) used in this experiment, the formation of the thermodynamically controlled product will occur rapidly [11]. The detection of the $Cu_6$-$\beta$ fragment following the proteolytic digestion of the whole protein reconstituted with 6 Cu(I) indicates that this thermodynamically controlled product involves Cu(I) binding to the $\beta$ domain [35]. The product formed after equilibration at high temperatures when 6 Cu(I) are added to $Zn_7$-MT can thus be represented as $(Zn_4)_\alpha(Cu_6)_\beta$-MT. The data in Fig. 3(A) show that the

luminescence from this $(Zn_4)_\alpha(Cu_6)_\beta$-MT species is much less than 50% of the luminescence from the $(Cu_6)_\alpha(Cu_6)_\beta$-MT species. Two possible explanations for this phenomenon are (i) differing degrees of solvent access in the two domains cause the Cu(I)–thiolate clusters in the $\alpha$ domain in the whole protein to emit more strongly than those in the $\beta$ domain or (ii) the peptide chain folds as the $(Cu_6)_\alpha(Cu_6)_\beta$-MT species forms so that the $\alpha$ and $\beta$ domains are close to each other thus blocking solvent to both domains. Either of these explanations should result in variations in the rate of luminescence quenching and in the rate of electron transfer.

The remainder of this work describes preliminary studies on the electron transfer and oxidative quenching reactions of $(Zn_4)_\alpha(Cu_6)_\beta$-MT and $(Cu_6)_\alpha(Cu_6)\beta$-MT. Experiments were carried out at high temperatures (40 °C) to ensure the presence of the fully equilibrated thermodynamically controlled products in all the protein complexes formed. Electron transfer reactions depend on the distance between the reactants; whereas collisional quenching reactions will depend on the degree of access to the emissive chromophore. Since both of these parameters will depend on the three-dimensional structure of the protein, the study of electron transfer and quenching rates can potentially yield novel information about the electronic structure of the Cu(I)–thiolate clusters.

### 3.2. Excited state lifetime measurements

In addition to the emission intensities, excited state lifetimes will also be affected by electron transfer reactions and collisional quenching. The relaxation process of an excited species D* can be explained by the function $[D]_t = [D]_0\{\Sigma A_i \exp(-t/\tau_i)\}$, where $[D]_t$ is the concentration of the species in its excited state at a given time, $[D]_0$ is the initial concentration, $\tau_i$ is the mean lifetime of the $i$th component and $A_i$ is the pre-exponential factor of that component. Previous lifetime data have been obtained by our group using the time-correlated, single-photon counting technique employed by the PRA model 3000 lifetime fluorometer [27] and by Beltramini et al. using frequency-domain phase and modulation measurements [36]. The detection methods used in these previous studies did not permit the determination of lifetimes >several $\mu$s; however, the LS-100 spectrometer can be used to determine longer lifetimes using boxcar integration with 1 $\mu$s channels. The results show that the data are best fit to curves described by a three-exponential function ($i=3$ in the above equation). With the temporal range extended to several 100 $\mu$s, we obtain the lifetimes given in Table 1 at 40 °C. Using time-resolved emission spectroscopy, we are able to isolate the luminescence spectrum due only to the longest-lived component of the emission ($\tau_1$ in Table 1). The quenching experiments described below were carried out using this time-resolved technique.

### 3.3. Electron transfer reactions

Electron transfer has recently been suggested as a possible biological role of metallothionein following the observation that Cd,Zn-MT can be used to reduce the heme protein ferricytochrome *c* [37]. The use of the Cd- and Zn-containing MT eliminates the possibility that the oxidation of the protein occurs through the metal centers as neither the Zn(II) nor the Cd(II) can be oxidized in aqueous solutions. A more likely mechanism involves irreversible oxidation of the cysteinyl thiolates. Indeed S-thiolation of the solvent-exposed cysteinyl ligands in $Zn_7$-MT by glutathione has been indicated in the release of zinc from metallothionein [38]. Oxidation of the cysteinyl sulfurs can lead to S–S crosslinking and the extrusion of the bound metals. The use of $Cu_{12}$-MT as a reducing agent instead of Zn- or Cd-MT, introduces another route for electron transfer as the Cu(I) centers can be readily oxidized.

Figs. 4 and 5 provide spectroscopic evidence that an electron transfer reaction takes place between $Cu_{12}$-MT and the Fe(III) in a potassium ferricyanide solution. In Fig. 4, absorption spectra obtained when equal volumes of a 36 mM potassium ferricyanide solution were added to either 2 ml of water or 2 ml of a solution 10 $\mu$M in $Cu_{12}$-MT at room temperature. The ligand to metal charge transfer bands of the $Fe(CN)_6^{3-}$ species in water alone located at 300 and 420 nm are replaced by a band gradually rising into the UV region in the presence of $Cu_{12}$-MT. The $Fe(CN)_6^{4-}$ species has virtually no absorption at 420 nm ($\epsilon = 2.1\ M^{-1}\ cm^{-1}$) and a weak band at 323 nm ($\epsilon = 345\ M^{-1}\ cm^{-1}$) which would be hidden under the protein absorption band [39]. These data clearly indicate that $Cu_{12}$-MT effectively reduces $Fe(CN)_6^{3-}$ to $Fe(CN)_6^{4-}$ ($E° = 0.36$ V [40]).

Fig. 5 shows the effect of the addition of potassium ferricyanide on the luminescence spectral properties of $Cu_{12}$-MT at 40 °C. As the $Fe(CN)_6^{3-}$ is added to $Cu_{12}$-MT, the emission intensity decreases until there is almost no intensity when 12 mol equiv. Fe(III) (based on moles Fe(III) per mole of metallothionein, i.e. per 20 cysteines or 12 Cu(I)) have been added. This decrease in luminescent intensity is accompanied by a collapse of the circular dichroism (CD) signal of $Cu_{12}$-MT. These data together show that the reduction of the Fe(III) is accompanied by oxidation of $Cu_{12}$-MT destroying the three-dimensional structure of the protein.

In addition to this classical electron transfer reaction, reversible electron transfer from the excited state of $Cu_{12}$-MT, which maintains the structure of the ground state, can also occur via collisional quenching. In this case, the presence of the triplet states of the Cu(I)

Table 1
Excited state lifetimes of $(Zn_4)_\alpha(Cu_6)_\beta$-MT and $(Cu_6)_\alpha(Cu_6)_\beta$-MT at 40 °C

| Sample | $\tau_1$ ($A_1$) ($\mu$s) | $\tau_2$ ($A_2$) ($\mu$s) | $\tau_3$ ($A_3$) ($\mu$s) |
|---|---|---|---|
| $Zn_7$-MT + 6 Cu(I) | 10 ± 1 (0.05 ± 0.01) | 3.0 ± 0.2 (0.16 ± 0.02) | 0.64 ± 0.05 (0.79 ± 0.03) |
| $Zn_7$-MT + 12 Cu(I) | 12 ± 2 (0.09 ± 0.05) | 3.60 ± 0.03 (0.38 ± 0.05) | 0.65 ± 0.05 (0.53 ± 0.04) |

The results represent the average of lifetimes and fractional components ($A_i$) obtained from decay curves from three different solutions at each Cu(I) concentration. The given error is the standard deviation associated with averaging the values calculated for each experiment.

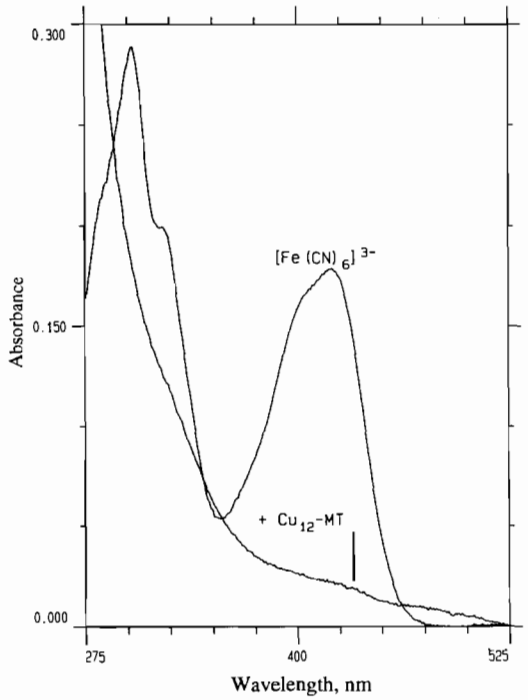


Fig. 4. Absorption spectra of potassium ferricyanide in the presence and absence of $Cu_{12}$-MT. Equal amounts of a 36 mM $K_3Fe(CN)_6$ solution were added to 2 ml of water and 2 ml of 10 $\mu$M $Cu_{12}$-MT and the absorption spectra recorded. The 300 and 420 nm charge transfer bands of $K_3Fe(CN)_6$ are not observed in the presence of $Cu_{12}$-MT.

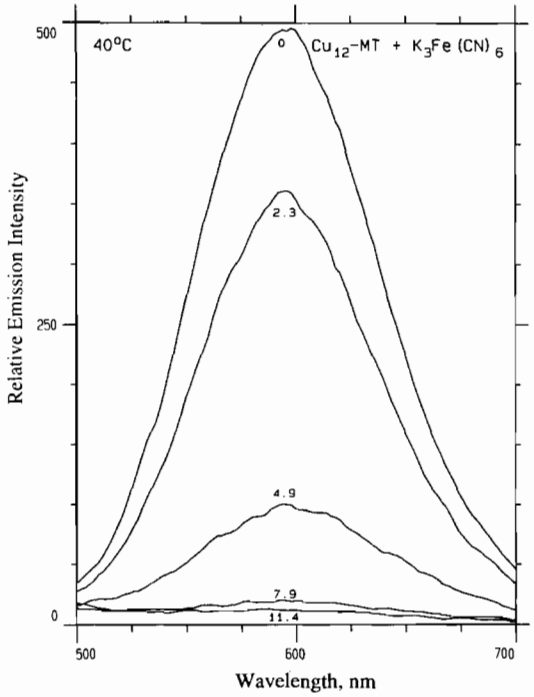


Fig. 5. Emission spectra recorded as potassium ferricyanide is added to $Cu_{12}$-MT at 40 °C. The lines represent the addition of 0, 2.3, 4.9, 7.9 and 11.4 mol equiv. of Fe(III) to the protein solution.

will enhance the oxidation potential of the Cu-MT towards reduction of an electron acceptor. Luminescence quenching is the technique of choice for examining these reactions.

### 3.4. Luminescence quenching

Molecular oxygen is perhaps the most common triplet quencher. In addition to quenching, the presence of oxygen may facilitate the oxidation of both the cysteine thiols and the Cu(I). Fig. 6 shows the effect of the presence of oxygen on the emission (Fig. 6(A) and (B)) and circular dichroism (CD) (Fig. 6(C) and (D)) spectra of solutions of $(Zn_4)_\alpha(Cu_6)_\beta$-MT, formed by adding 6 Cu(I) (Fig. 6(A) and (C)) and $(Cu_6)_\alpha(Cu_6)_\beta$-MT, formed by adding 12 Cu(I) to $Zn_7$-MT, (Fig. 6(B) and (D)). The stated amount of Cu(I) solution was added to an argon-saturated solution of $Zn_7$-MT equilibrated at 40 °C and the solution was further purged with argon for 5 min. After 1 h in a sealed cuvette at 40 °C, the solution was again bubbled with argon for 5 min before recording the emission and CD spectra (line a in Fig. 6(A)–(D)). The solutions were then bubbled with compressed air for 15 min, allowed to equilibrate with the atmosphere and the emission and CD spectra recorded (line b in Fig. 6(A)–(D)). Based on Henry's law constant of $5.325 \times 10^4$ atm for oxygen dissolved in water at 313 K as calculated from the smoothing equation described in Ref. [41] and a partial pressure of oxygen of 0.21 atm in a normal dry atmosphere, the concentration of oxygen dissolved in these aerated solutions was approximately 0.22 mM. After re-saturating the solutions with argon for 15 min, the emission and CD spectra were recorded again (line c in Fig. 6(A)–(D)).

The data in Fig. 6 clearly indicates that the excited state in both $(Zn_4)_\alpha(Cu_6)_\beta$-MT and $(Cu_6)_\alpha(Cu_6)_\beta$-MT

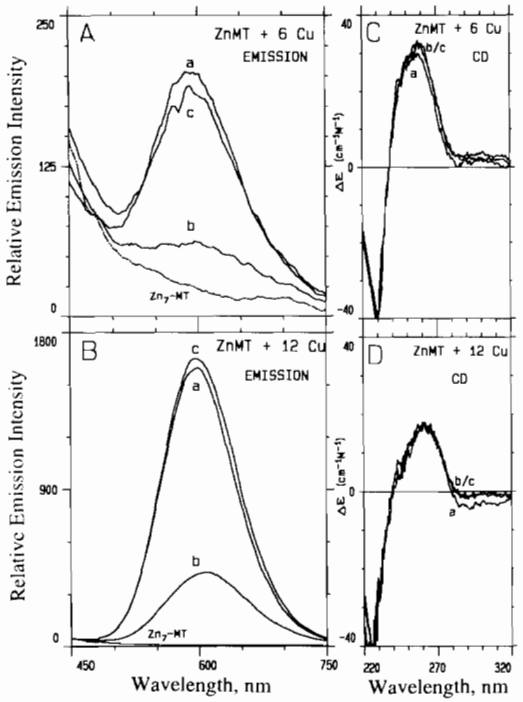


Fig. 6. Emission (A and B) and circular dichroism (C and D) spectra recorded as argon-saturated solutions of copper-containing metallothioneins are saturated with air and then re-saturated with argon. (A) and (C) show the spectra obtained from a solution of 10 $\mu$M $Zn_7$-MT mixed with 6 Cu(I); (B) and (D) show the spectra obtained from a solution of 10 $\mu$M $Zn_7$-MT mixed with 12 Cu(I). Line a in all four plots indicates the original spectrum of the argon-saturated solutions, line b represents the spectrum obtained after saturating the solutions with air, and line c represents the spectrum obtained when the solutions are re-saturated with argon. The dashed line in A and B is the emission spectrum of $Zn_7$-MT alone.

are efficiently and reversibly quenched by molecular oxygen. Oxidation of both cysteinyl thiols and Cu(I) is a common and expected reaction of a copper-containing sulfur-rich protein. The standard electrode potential ($E°$) for the Cu(II)/Cu(I) couple is 0.159 V in aqueous solution [42] and the electrode potential for RS–SR/RSH systems at pH 7 is in the range of $-0.38$ V [43]. Because the three-dimensional structure of the copper binding site is entirely dependent on the presence of the interlocking system of Cu–S bonds, oxidation of either the thiolate to disulfide or Cu(I) to Cu(II) will result in irreversible full or partial demetallation of the metallothionein causing major changes in the overall three-dimensional structure of the protein. This would produce drastic and irreversible changes in both the CD and emission spectra. In the absence of chemical oxidation, only the emission spectrum would be affected by the luminescent quenching abilities of the oxygen. Significantly, the data in Fig. 6 show that the presence of oxygen has no effect on the CD spectra of copper-substituted metallothioneins and that the effect of oxygen on the emission spectra is completely reversible. This indicates that no chemical oxidation of either the cysteine thiols or the Cu(I) atoms has occurred. Molecular oxygen acts only as an excited state quenching agent. Even solutions that have been exposed to air over 12 h have their luminescent intensity regenerated by de-aerating with argon. This result is especially significant in terms of the explanation of the unusual dependence of the emission quantum yield on the Cu(I):MT molar ratio shown in Fig. 3 and more fully described by us previously [11].

We can further analyze the effect of oxygen quenching as shown in Fig. 6 in terms of the bimolecular rate of quenching. The rate of deactivation of an excited species X* through collisional quenching by Q is given by the expression $k_q[X^*][Q]$ where $k_q$ is the bimolecular quenching rate constant. This rate constant can be computed from the Stern–Volmer equation $F_0/F = 1 + k_q\tau_0[Q]$ where $F_0$ is the emission intensity without quencher, $F$ is the emission intensity at a quencher concentration of [Q] and $\tau_0$ is the fluorescence lifetime of X* in the absence of the quencher. The quantity $k_q\tau_0$ ($K_{SV}$ – the Stern–Volmer constant) can be obtained from the initial slope of a linear Stern–Volmer plot of $F_0/F$ versus [Q]. $k_q$ for $O_2$ quenching of *Neurospora crassa* Cu-MT (a smaller metallothionein with a single copper binding domain that is similar in structure to the $\beta$ domain of mammalian Cu-MT [2]) has been reported as $6.6\times10^8$ $M^{-1}$ $s^{-1}$ at 10 °C [36]. Our results for the quenching of mammalian Cu-MT by molecular oxygen at 40 °C give $K_{SV}$ of $9.88\times10^3$ $M^{-1}$ and $1.26\times10^4$ $M^{-1}$ for $(Zn_4)_\alpha(Cu_6)_\beta$-MT and $(Cu_6)_\alpha(Cu_6)_\beta$-MT, respectively. Based on a $\tau_0$ of $\sim10$ $\mu$s ($\tau_1$ in Table 1), the $k_q$ values for oxygen quenching of both mammalian Cu-MT species is approximately $10^9$ $M^{-1}$ $s^{-1}$, an order of magnitude lower than the rate constant for a diffusion-controlled process. The similarity in the values of $k_q$ for oxygen quenching is not unexpected. The penetration, or insertion, of molecular oxygen into proteins to quench the fluorescence of buried tryptophans has been previously reported [44]. This quenching occurs at a rate slightly lower than the free solvent diffusional limit, independent of the solvent exposure of the luminophores [44]. While the rate of quenching by molecular oxygen clearly cannot yield any structural information, these luminescence data confirm the chemical, electronic and structural stability of the copper–thiolate clusters. Indeed, these data provide evidence for the presence of molecular orbitals that span all 6 Cu(I) in each cluster because the emission intensity is totally quenched by the oxygen. The use of a larger contact quencher, such as acrylamide, which cannot penetrate into the protein may provide information on solvent accessibility to the copper–thiolate clusters.

Figs. 7(A) and 8 show Stern–Volmer plots calculated from data obtained when acrylamide was added to $(Zn_4)_\alpha(Cu_6)_\beta$-MT and $(Cu_6)_\alpha(Cu_6)_\beta$-MT at 40 °C, respectively. The Stern–Volmer plot of the acrylamide

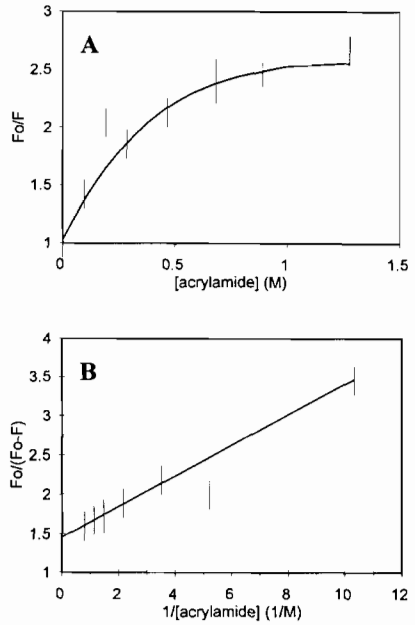


Fig. 7. Stern–Volmer plots for the acrylamide quenching of $(Zn_4)_\alpha(Cu_6)_\beta$-MT at 40 °C. The data points are shown by bars which represent the error in three measurements on the same solution. In A, the unquenched emission intensity ($F_0$) divided by the quenched emission intensity is plotted vs. the acrylamide concentration. The solid line shows the downward curvature at high acrylamide concentrations. In B, the unquenched emission intensity ($F_0$) divided by the difference in quenched and unquenched intensities ($F_0-F$) is plotted vs. the inverse concentration of acrylamide. The line represents the best fit line calculated by least-squares regression analysis.

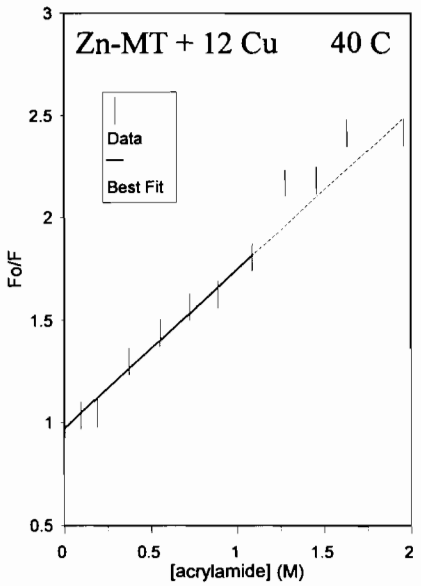


Fig. 8. Stern–Volmer plot for the acrylamide quenching of $Cu_{12}$-MT at 40 °C. The unquenched emission intensity ($F_0$) divided by the quenched emission intensity is plotted vs. the acrylamide concentration. The data points are shown by bars which represent the error in five measurements on the same solution. The solid line represents the calculated best fit line though the first seven points (at lower acrylamide concentrations). The dashed line is an extrapolation of this line to higher acrylamide concentrations.

quenching of $(Zn_4)_\alpha(Cu_6)_\beta$-MT (Fig. 7(A)) exhibits a downward curvature at high quencher concentrations; whereas the Stern–Volmer plot for the acrylamide quenching of $(Cu_6)_\alpha(Cu_6)_\beta$-MT (Fig. 8) is linear. $K_{SV}$ for the acrylamide quenching of $(Cu_6)_\alpha(Cu_6)_\beta$-MT can be determined directly from the slope of the plot in Fig. 8, but the data in Fig. 7(A) must be replotted according to a modified Stern–Volmer equation (Fig. 7(B)). $F_0/(F_0-F)$ plotted against $[Q]^{-1}$ will yield a straight line where the intercept/slope is the effective Stern–Volmer constant and 1/intercept is the maximum fraction of accessible fluorescence ($f_a$) [45]. From such a plot (Fig. 7(B)), $K_{SV}$ for the acrylamide quenching of $(Zn_4)_\alpha(Cu_6)_\beta$-MT is 7.5 $M^{-1}$, resulting in a $k_q$ value of $7.5\times10^5$ $M^{-1}$ $s^{-1}$. Fig. 8, on the other hand, yields a $K_{SV}$ value for the acrylamide quenching of $(Cu_6)_\alpha(Cu_6)_\beta$-MT at 40 °C of 0.78 $M^{-1}$, resulting in a $k_q$ value of $6.5\times10^4$ $M^{-1}$ $s^{-1}$. It should be noted that a plot of $F_0/\Delta F$ versus $[Q]^{-1}$ of these data (not shown) yields a similar value of $K_{SV}$ (0.70 $M^{-1}$) and a value of $f_a$ close to 1. This indicates that in $(Cu_6)_\alpha(Cu_6)_\beta$-MT each luminophore must be subject to a similar degree of fluorescence quenching (i.e. either equally accessible or equally shielded) [45]. From Fig. 7(B), the value of $f_a$ is 0.69, indicating that only two-thirds of the luminophores are being quenched by the acrylamide and that one-third of the luminophores are more deeply buried [45].

The values of $k_q$ for the acrylamide quenching of both $(Zn_4)_\alpha(Cu_6)_\beta$-MT and $(Cu_6)_\alpha(Cu_6)_\beta$-MT are four or five orders of magnitude lower than the corresponding values of $k_q$ for the quenching by molecular oxygen. This is to be expected in the case of non-exposed luminophores [44]. The fact that $k_q$ for the acrylamide quenching of $(Cu_6)_\alpha(Cu_6)_\beta$-MT is an order of magnitude lower than that for $(Zn_4)_\alpha(Cu_6)_\beta$-MT verifies our previous conclusions of lowered solvent accessibility in the $(Cu_6)_\alpha(Cu_6)_\beta$-MT species. As stated previously, this lowered solvent accessibility could either be caused by lower solvent accessibility to the copper–thiolate clusters in the $\alpha$ domain than to those in the $\beta$ domain or by folding of the peptide chain during the formation of the $(Cu_6)_\alpha(Cu_6)_\beta$-MT species so that the $\alpha$ and $\beta$ domains are close to each other, effectively blocking both domains from the solvent. The published $k_q$ for the acrylamide quenching of *Neurospora crassa* Cu-MT is $3.8\times10^6$ $M^{-1}$ $s^{-1}$ at 10 °C [36]. This may indicate that the luminophores in the two domain mammalian copper metallothioneins are less exposed than those in the one domain of *Neurospora crassa* Cu-MT, although the differing experimental temperatures makes drawing definitive conclusions difficult.

## 4. Conclusions

(1) Cu-MT is active in electron transfer as monitored by luminescence quenching.

(2) CD spectral properties show that the three-dimensional structure of the protein is maintained even when the excited state is completely quenched by molecular oxygen.

(3) Different acrylamide quenching rates of $(Zn_4)_\alpha(Cu_6)_\beta$-MT and $(Cu_6)_\alpha(Cu_6)_\beta$-MT indicate that structural differences dependent on the Cu(I) loading influence the excited state properties of copper-containing mammalian metallothioneins.

(4) Fe(III) is efficiently reduced to Fe(II) following oxidative quenching of the luminescence of $Cu_{12}$-MT; CD spectroscopy shows that the three-dimensional structure of $Cu_{12}$-MT is destroyed.

## Acknowledgements

We acknowledge useful discussions with Anthony Presta at U.W.O. and the assistance of John Dixon at U.W.O. with data presentation. We gratefully acknowledge financial support of this work from the Natural Sciences and Engineering Research Council of Canada for an operating grant (to M.J.S.) and a Graduate Scholarship (to A.R.G.), and from the Academic Development Fund at the U.W.O. for an equipment grant (to M.J.S.). We also thank the Center for Chemical Physics at U.W.O. for continued support of our work. M.J.S. is a member of the Center for Chemical Physics and the Photochemistry Unit at U.W.O. This is publication number 507 of the Photochemistry Unit.

## References

[1] M.J. Stillman, C.F. Shaw III and K.T. Suzuki (eds.), *Metallothioneins,* VCH, New York, 1992.
[2] J.H.R. Kagi and Y. Kojima (eds.), *Metallothionein II,* Birkhauser, Basel, Switzerland, 1987; Exp. Suppl. 52.
[3] P.E. Hunziker and J.H.R. Kagi, in P.M. Harrison (ed.), *Metalloproteins – Part II: Metal Proteins with Non-redox Roles,* Macmillan, London, 1985, pp. 149–182.
[4] M.J. Stillman, in M.J. Stillman, C.F. Shaw III and K.T. Suzuki (eds.), *Metallothioneins,* VCH, New York, 1992, Ch. 4, pp. 55–127.
[5] J.D. Otvos and I.M. Armitage, *Proc. Natl. Acad. Sci. U.S.A., 77* (1980) 7094–7098.
[6] B.A. Messerle, A. Schaffer, M. Vasak, J.H.R. Kagi and K. Wuthrich, *J. Mol. Biol., 225* (1992) 433–443.
[7] A.H. Robbins, D.E. McRee, M. Williamson, S.A. Collett, N.H. Xuong, W.F. Furey, B.C. Wang and C.D. Stout, *J. Mol. Biol., 221* (1991) 1269–1293.
[8] A.H. Robbins and C.D. Stout, in M.J. Stillman, C.F. Shaw III and K.T. Suzuki (eds.), *Metallothioneins,* VCH, New York, 1992, Ch. 3, pp. 31–54.
[9] I.J. Pickering, G.N. George, C.T. Dameron, B. Kurz, D.R. Winge and I.G. Dance, *J. Am. Chem. Soc., 115* (1993) 9498–9505.
[10] W. Lu and M.J. Stillman, *J. Am. Chem. Soc., 115* (1993) 3291–3299.
[11] A.R. Green, A. Presta, Z. Gasyna and M.J. Stillman, *Inorg. Chem., 33* (1994) 4159–4168.
[12] A. Presta, A.R. Green, A. Zelazowski and M.J. Stillman, *Eur. J. Biochem.,* submitted for publication.
[13] K.B. Nielson, C.L. Atkin and D.R. Winge, *J. Biol. Chem., 260* (1985) 5342–5350.
[14] A.J. Zelazowski and M.J. Stillman, *Inorg. Chem., 31* (1992) 3363–3370.
[15] W. Cai and M.J. Stillman, *J. Am. Chem. Soc., 110* (1988) 7872–7873.
[16] W. Lu, A.J. Zelazowski and M.J. Stillman, *Inorg. Chem., 32* (1993) 919–926.
[17] G.N. George, D.R. Winge, C.D. Stout and S.P. Cramer, *J. Inorg. Biochem., 27* (1986) 213–220.
[18] I.L. Abrahams, I. Bremner, G.P. Diakun, C.D. Garner, S.S. Hasnain, I. Ross and M. Vasak, *Biochem. J., 236* (1986) 585–589.
[19] M. Beltramini and K. Lerch, *FEBS Lett., 127* (1981) 201–203.
[20] J.A. Szymanska, A.J. Zelazowski and M.J. Stillman, *Biochem. Biophys. Res. Commun., 115* (1983) 167–173.
[21] M.J. Stillman and J.A. Szymanska, *Biophys. Chem., 19* (1984) 163–169.
[22] K. Munger and K. Lerch, *Biochemistry, 24* (1985) 6751–6756.
[23] K. Munger, U.A. Germann, M. Beltramini, D. Niedermann, G. Baitella-Eberle, J.H.R. Kagi and K. Lerch, *J. Biol. Chem., 260* (1985) 10032–10038.
[24] R.K. Mehra and I. Bremner, *Biochem. J., 219* (1984) 539–546.
[25] R.N. Reese, R.K. Mehra, E.B. Tarbet and D.R. Winge, *J. Biol. Chem., 263* (1988) 4186–4192.
[26] J. Byrd, R.M. Berger, D.R. McMillin, C.F. Wright, D. Hamer and D.R. Winge, *J. Biol. Chem., 263* (1988) 6688–6694.
[27] (a) Z. Gasyna, A. Zelazowski, A.R. Green, E.A. Ough and M.J. Stillman, *Inorg. Chim. Acta, 153* (1988) 115–118; (b) M.J. Stillman and Z. Gasyna, *Methods in Enzymol., 205* (1991) 540–555.
[28] M.J. Stillman, W. Cai and A.J. Zelazowski, *J. Biol. Chem., 262* (1987) 4538–4548.
[29] A.J. Zelazowski, J.A. Szymanska and H. Witas, *Prep. Biochem., 10* (1980) 495–505.
[30] (a) G.L. Ellman, *Arch. Biochem. Biophys., 82* (1959) 70–77; (b) W. Birchmeier and P. Christen, *FEBS Lett., 18* (1971) 209–213.
[31] P. Hemmerich and C. Sigwart, *Experientia, 19* (1963) 488–489.
[32] Z. Gasyna, W.R. Browett, T. Nyokong, B. Kitchenham and M.J. Stillman, *Chemom. Intell. Lab. Syst., 5* (1989) 233–246.
[33] (a) W.R. Browett and M.J. Stillman, *Comput. Chem., 11* (1987) 73–80; (b) J.A. Dixon and M.J. Stillman, unpublished program.
[34] Y.-J. Li and U. Weser, *Inorg. Chem., 31* (1992) 5526–5533.
[35] K.B. Nielson and D.R. Winge, *J. Biol. Chem., 259* (1984) 4941–4946.
[36] M. Beltramini, G.M. Giacometti, B. Salvato, G. Giacometti, K. Munger and K. Lerch, *Biochem. J., 260* (1989) 189–193.
[37] C. Simpkins, P. Eudaric, C. Torrence and Z. Yang, *Life Sci., 53* (1993) 1975–1980.
[38] W. Maret, *Proc. Natl. Acad. Sci. U.S.A., 91* (1994) 237–241.
[39] A.B.P. Lever, *Inorganic Electronic Spectroscopy,* Elsevier, New York, 1968, p. 302.
[40] F.A. Cotton and G. Wilkinson, *Advanced Inorganic Chemistry,* Wiley, Toronto, 5th edn., 1988, p. 714.
[41] B.B. Benson, D. Krause and M.A. Peterson, *J. Solution Chem., 8* (1979) 655–690.

[42] U. Bertocci and D.D. Wagman, in A.J. Bard, R. Parsons and J. Jordan (eds.), *Standard Potentials in Aqueous Solution*, Marcel Dekker, New York, 1985, Ch. 11-I, pp. 287–293.

[43] W.M. Clark, *Oxidation–Reduction Potentials of Organic Systems*, Robert E. Krieger, Huntington, NY, 1972, pp. 471–487.

[44] D.B. Calhoun, J.M. Vanderkooi, G.R. Holtom and S.W. Englander, *Proteins, 1* (1986) 109–115.

[45] S.S. Lehrer, *Biochemistry, 10* (1971) 3254–3263.

[46] J.H.R. Kagi, in K. Suzuki, N. Imura and M. Kimura (eds.), *Metallothionein III*, Birkhauser, Basel, Switzerland, 1993, pp. 29–56.